Journal of Sound and Vibration (2001) **243**(5), 775–796
doi:10.1006/jsvi.2000.3477, available online at http://www.idealibrary.com on IDEAL®

PRESSURE CALCULATION IN A COMPRESSOR CYLINDER BY A MODIFIED NEW HELMHOLTZ MODELLING

Y.-C. MA

Ray W. Herrick Laboratories, School of Mechanical Engineering, Purdue University, IN, U.S.A.
E-mail: ycma@ecn.purdue.edu

AND

O.-K. MIN

Department of Mechanical Design and Production Engineering, Yonsei University, Seoul, South Korea

(*Received* 11 *October* 1999, *and in final form* 8 *August* 2000)

Pressure pulsation has a critical importance in the design of refrigerant compressor since it affects the performance by increasing over-compression loss, and it acts as a noise and vibration source. For the numerical analysis of pressure pulsation, quasi-steady flow equation has been used because of its easy manipulation derived from the pressure difference. By considering the dynamic effects of fluid, a new Helmholtz resonator model was also proposed on the basis of the continuity and the momentum equations, which consists of necks and cavities in flow manifolds.

In this paper, a modified new Helmholtz resonator is introduced to include the gas inertia effect due to the volume decrease in the cavity. Comparisons between this modified new Helmholtz calculations and experimental results show that it is necessary to include the gas inertia effect in predicting pressure over-shooting phenomena at an instant of valve opening state and this modified new Helmholtz model can describe the over-compression phenomena in the compressor cylinder, a phenomenon which hinders a noise source identification of compressor.

1. INTRODUCTION

1.1. GENERAL

Noise and vibration control of hermetic-type compressors should start with the identification of the sources of noise and vibration. The coupling between the compressor structure and the working fluid is a key mechanism in noise generated by systems. This type of coupling, which makes the pressure pulsation characteristics important, is typical of fluid dynamic systems where machinery is involved. Pressure pulsations have critical importance in the design of refrigerant compressors since they affect the performance by increasing losses related to over-compression, and they also act as a noise and vibration source. For the numerical analysis of pressure pulsations, a new modified Helmholtz Resonator model is introduced here to include the gas inertia effect due to the volume decrease in the cavity. This new model can describe the over-compression phenomena in the compressor cylinder, a phenomenon which hinders a noise source identification of the compressor.

0022-460X/01/250775 + 22 $35.00/0

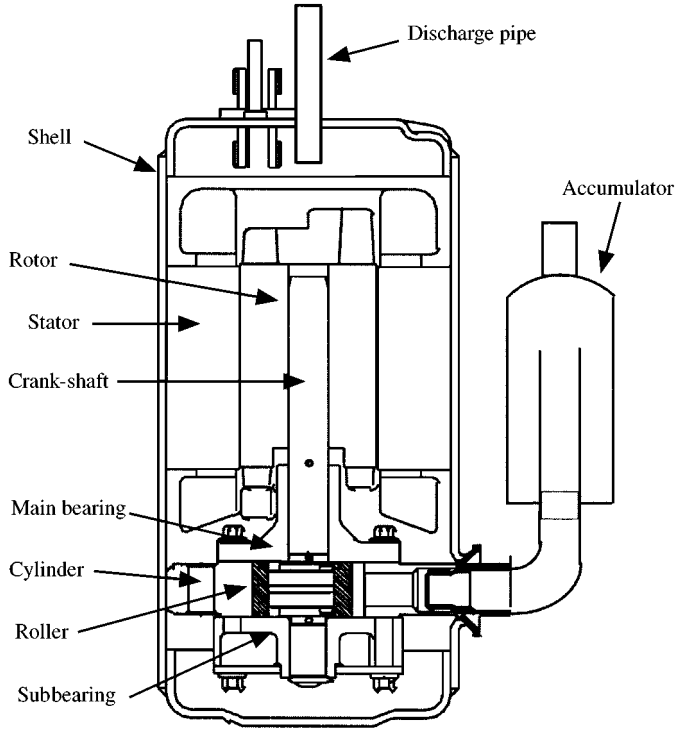

Figure 1. Rolling piston type rotary compressor.

1.1.1. *The cause of pressure pulsation*

Unsteady flows in suction and discharge pipes are generated by the reciprocating action of the piston, aided by the rapid opening and closing of pressure-actuated valves. These pressure fluctuations, in turn, affect valve displacements, cylinder pressure and instantaneous fluid flow rates. Pressure pulsation consists of a steady fluctuation due to the periodical motion of refrigerant gas during the suction and discharging process, and a transient pulsation due to the valve motion which controls the discharge of the compressed refrigerant gas.

1.1.2. *Definition and role of a cylinder*

Among hermetic compressors, a rolling piston type rotary compressor in Figure 1 has a lot of components.

The compressor cylinder is a chamber where a suction and compression cycle of a refrigerant gas occurs, and chamber volume varies according to the compression process due to a roller rotation. Therefore, the state of temperature and pressure of a refrigerant gas changes from a low to high state. The volume V of a compression chamber of the cylinder in Figure 2 is described by following geometrical relations as a function of rotating angle θ [1].

$$V(\theta) = V_T - \tfrac{1}{2} R_C^2 H_c \theta + \tfrac{1}{2} R_R^2 H_c(\theta + \alpha) + \tfrac{1}{2} e H_c (R_R + R_V) \sin(\theta + \alpha)$$

$$- \tfrac{1}{2} R_v^2 H_c \tan(\theta + \alpha) - \tfrac{1}{2} b H_c \chi, \tag{1}$$

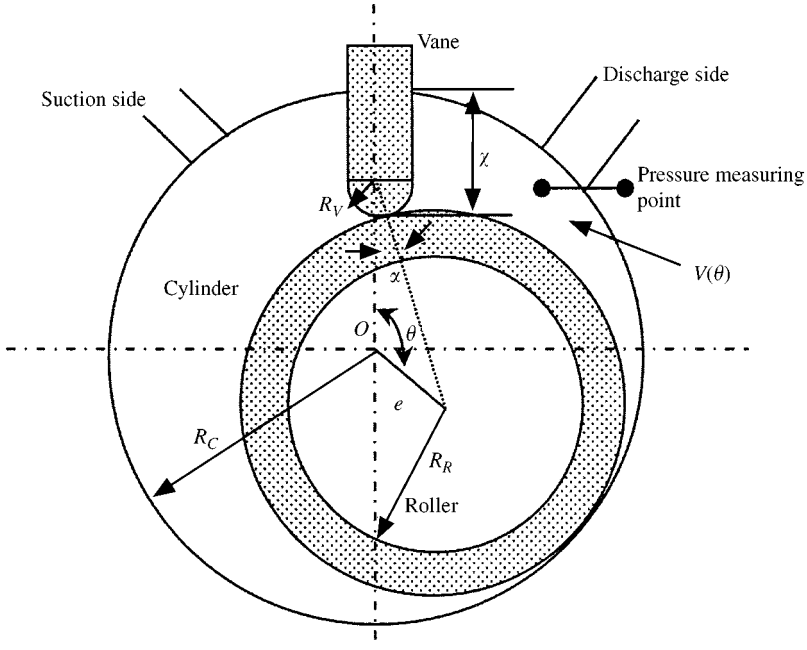

Figure 2. Sectional view of cylinder in a rotary-type compressor.

where

$$V_T = \pi(R_C^2 - R_R^2), \quad \alpha = \sin^{-1}\left(\frac{e}{R_R + R_V}\sin\theta\right), \quad \chi = R_C + R_V - (R_R + R_V)\cos\alpha - e\cos\theta.$$

Here V_T is the total volume of a compressor cylinder, H_c the cylinder height, b the vane thickness, R_V the vane tip radius, χ the vane extension, R_R the roller radius, R_C the cylinder radius, and e the relative eccentricity $(R_C - R_R)$.

Volume flow rate of a cylinder can also be represented as follows:

$$\frac{dV(\theta)}{dt} = \frac{1}{2}(R_R - R_C)H_c\omega + \frac{1}{2}R_R^2 H_c\frac{d\alpha}{dt} + \frac{1}{2}eH_c(R_R + R_V)\cos(\theta + \alpha)\left(\omega + \frac{d\alpha}{dt}\right)$$
$$- \frac{1}{2}R_V^2 H_c \sec^2\alpha\frac{d\alpha}{dt} - \frac{1}{2}bH_c\frac{d\chi}{dt}, \tag{2}$$

where

$$\frac{d\alpha}{dt} = \frac{e\omega\cos\theta}{R_R + R_V}\left[1 - \left(\frac{e}{R_R + R_V}\sin\theta\right)\right]^{-1/2},$$

$$\frac{d\chi}{dt} = (R_R + R_V)\sin\alpha + e\omega\sin\theta.$$

1.2. THE CALCULATION METHOD OF PRESSURE PULSATION IN A CYLINDER

A lot of studies of the pressure calculation of a compressor cylinder has been reported, namely a quasi-steady (QS), classical Helmholtz resonator (CHR), and new Helmholtz

resonator (NHR). These conventional methods are summarized briefly below for a comparison with our proposed method (MNHR).

1.2.1. *Quasi-steady* (*QS*) [2]

The general calculation method of the pressure of a cylinder is a quasi-steady flow equation. This method calculates the mass flow rate due to the pressure difference between upstream and downstream sides, and it is convenient to obtain the density and pressure without the calculation of fluid velocity. These relations are shown in Table A1 of Appendix A.

However, it is not sufficient for this method to describe a dynamic response of pressure pulsation since it disregards the dynamic behaviour of fluid.

1.2.2. *Classical Helmholtz resonator* (*CHR*) [3]

The CHR approximation was proposed as a new convenient approach. The gas is considered to have inertia only in the necks (or connecting passages) and to be inertialess in the cavities (or plenums) because of the relative differences in accelerating levels. On the other hand, the gas is considered to be compressible in the cavities, but incompressible in the neck because of the relative differences in volume. One may, therefore, picture the acoustic model as consisting of incompressible plugs of gas in the necks, that oscillate like pistons on springs that are provided by the elasticity of the compressible gas in the cavities.

1.2.3. *New Helmholtz resonator* (*NHR*) [4, 5]

Another simplified method is NHR, which has the same assumption of the CHR described above. However, CHR assumes that pressure and velocity amplitudes are small, and all densities are constant, and introduce bulk modulus of elasticity which represents a value of the density times the sound speed squared. But NHR distinguishes a difference of densities at control volumes, all densities are thus not constant. The density of a neck is also obtained by averaging those of the cavities.

1.2.4. *Modified new Helmholtz resonator* (*MNHR*)

This method is a new proposed calculation approach, to consider a gas inertia effect due to the volume decrease of this cylinder, which is not included in these conventional methods mentioned above (QS, CHR, NHR).

2. FORMULATION FOR A DEFORMABLE VOLUME

For the calculation of cylinder pressure using control volume approach, a model of deformable and moving control volume is introduced since the volume of cylinder structure is varying during compressor operation.

2.1. THE MOTION EQUATION IN A DEFORMABLE CONTROL VOLUME

The fundamental laws governing the motion of a fluid are generally Lagrangian descriptions; however, when a particular group of particles is not of fundamental interest, Eulerian descriptions are used, which define a region in space called a control volume and observe the fluid flowing through it. Therefore, we introduce a mathematical description of

fluid motion equation on a deformable and moving control volume, from the Eulerian point of view [6].

Let N_{sys} be the extensive property in system. It would be calculated by integrating its corresponding intensive property η over the volume of interest, that is,

$$N_{sys} = \int_V \eta\rho \,\mathrm{d}V, \tag{3}$$

where η is N_{sys} per unit mass. The time rate of change of N_{sys} is

$$\frac{\mathrm{D}(N_{sys})}{\mathrm{D}t} = \frac{\mathrm{D}}{\mathrm{D}t}\int_{sys} \eta\rho \,\mathrm{d}V = \lim_{\Delta t \to 0} \frac{N_{sys}(t+\Delta t) - N_{sys}(t)}{\Delta t}. \tag{4}$$

The deformable control volume differs from the fixed control volume in that the control boundary is allowed to move, as for a reciprocating piston. A system including control volume moves and deforms from arbitrary time t to $t + \Delta t$, and this relation and defining terms for the following derivation below are presented in Figure 3.

Relative velocity effects between a system and a control volume are described when both move and deform. The system boundaries move at velocity $\mathbf{u}$, and the control surface moves at velocity $\mathbf{u}_b$. The relative velocity $\mathbf{u}_r$ thus occurs between the fluid system and the control surface.

The system and control volume are coincident at time t. At time $t + \Delta t$, the system will have translated and deformed and the control volume will also have translated and deformed, but differently from the system

Referring to Figure 3, $N_{sys}(t + \Delta t)$ and $N_{sys}(t)$ may then be written as follows:

$$N_{sys}(t+\Delta t) = N_5(t+\Delta t) + N_4(t+\Delta t) + N_3(t+\Delta t), \tag{5a}$$

$$N_{sys}(t) = N_3(t) + N_2(t) + N_1(t). \tag{5b}$$

Substituting these equations (5a, b) into equation (4) and we have

$$\frac{\mathrm{D}(N_{sys})}{\mathrm{D}t} = \lim_{\Delta t \to 0}\left[\frac{N_5(t+\Delta t) + N_4(t+\Delta t) + N_3(t+\Delta t) - N_3(t) - N_2(t) - N_1(t)}{\Delta t}\right]. \tag{6}$$

To get the desired form, $N_6(t + \Delta t)$; a summed region (2), (A) and (B) in Figure 3, is added and subtracted as follows:

$$\frac{\mathrm{D}(N_{sys})}{\mathrm{D}t} = \lim_{\Delta t \to 0}\left[\frac{N_4(t+\Delta t) + N_3(t+\Delta t) + N_6(t+\Delta t) - N_3(t) - N_2(t) - N_1(t)}{\Delta t} + \frac{N_5(t+\Delta t) - N_6(t+\Delta t)}{\Delta t}\right]. \tag{7}$$

The first term on the right-hand side of equation (7) above means the time-rate-of-change in control volume, and the second term is arranged using the differential volume element in regions (5) and (6).

Referring again to Figure 3, equation (7) above therefore may be written as

$$\frac{\mathrm{D}(N_{sys})}{\mathrm{D}t} = \lim_{\Delta t \to 0}\frac{N_{cv}(t+\Delta t) - N_{cv}(t)}{\Delta t} + \lim_{\Delta t \to 0}\frac{N_5(t+\Delta t) - N_6(t+\Delta t)}{\Delta t}.$$

$$= \frac{\mathrm{d}}{\mathrm{d}t}\left(\int_{cv} \eta\rho \,\mathrm{d}V\right) + \lim_{\Delta t \to 0}\frac{1}{\Delta t}\left\{\int_{A_5} \eta\rho(\mathbf{u}_r \cdot \mathbf{n})\,\mathrm{d}A\Delta t - \int_{A_6} \eta\rho(-\mathbf{u}_r \cdot \mathbf{n})\,\mathrm{d}A\Delta t\right\}, \tag{8}$$

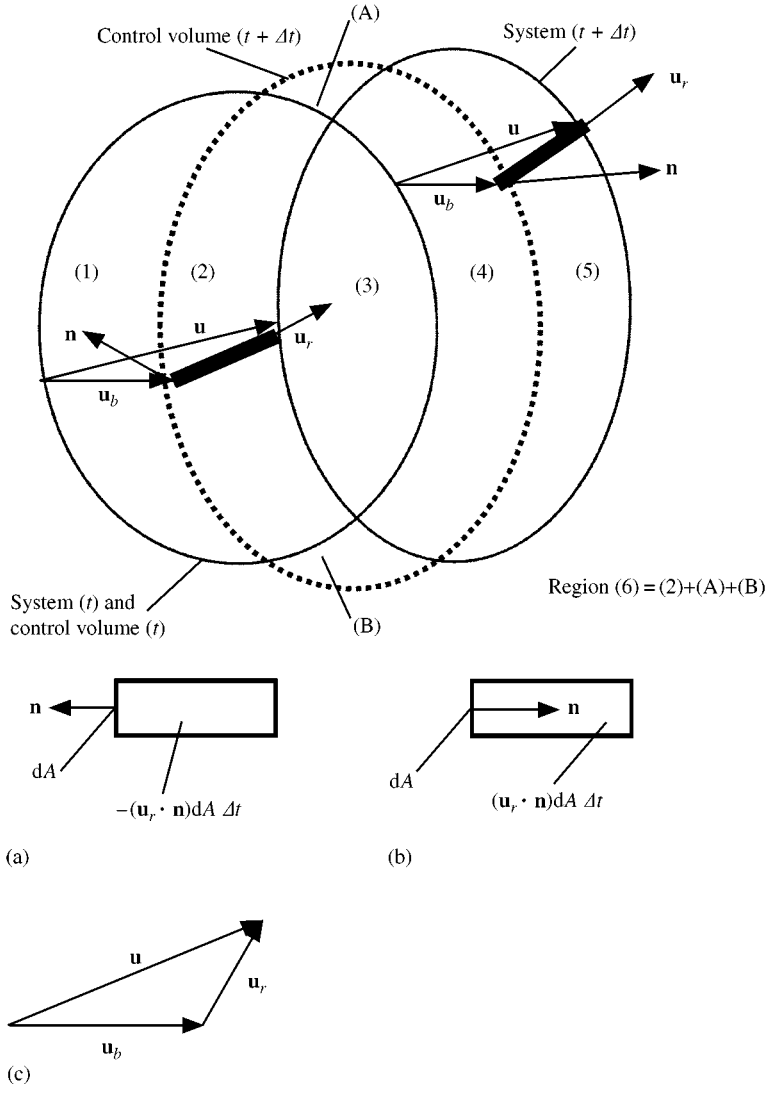

Figure 3. The system and the deformable control volume: (a) Element volume from region (6); (b) element volume from region (5); and (c) velocity polygon. $\mathbf{u}$ is the velocity of fluid element; $\mathbf{u}_r$ the relative velocity with respect to control-volume boundary; $\mathbf{u}_b$ the velocity of control-volume boundary.

where $\mathbf{u}_r$ in Figure 3 represents the velocity of the fluid relative to control volume between the control volume and system at time $t + \Delta t$, and $\mathbf{n}$ in Figure 3 always points out of the control volume. Equation (8) can be represented as

$$\frac{\mathrm{D}}{\mathrm{D}t}(N_{sys}) = \frac{\mathrm{d}}{\mathrm{d}t}\left(\int_{cv} \eta\rho \,\mathrm{d}V\right) + \int_{cs} \eta\rho\,(\mathbf{u}_r \cdot \mathbf{n})\,\mathrm{d}A. \tag{9}$$

This is often referred to as the Reynolds transport theorem. D/Dt on the left-hand side means that we are following a particular group of fluid particles, and d/dt on the right-hand side also used since we are only looking at a volume in space and not particular particles. The first term on the right-hand side is referred to as the time-rate-of-change term and the

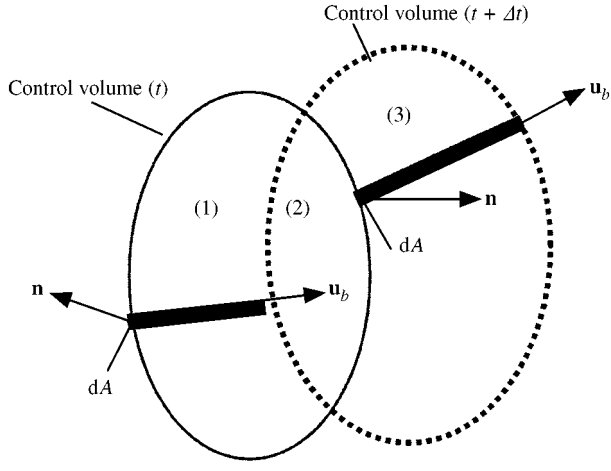

Figure 4. The deformable control volume.

second as the flux one. Subscripts *cs* in equation (9) represents the control surface, which completely encloses the control volume.

The time-rate-of-change term of the basic system-to-control-volume transformation may be reformulated to more easily account for the rate of deformation. Consider a generalized control volume at time t and let it deform, assuming the position shown in Figure 4 at time $t + \Delta t$. Referring to Figure 4, and the same procedure for the derivation of equation (9) above, the time-rate-of-change term is reformulated as follows:

$$\frac{\mathrm{d}}{\mathrm{d}t}\int_{cv}\eta\rho\,\mathrm{d}V = \frac{\mathrm{d}N_{cv}}{\mathrm{d}t} = \lim_{\Delta t\to 0}\frac{N_{cv}(t+\Delta t) - N_{cv}(t)}{\Delta t}$$

$$= \lim_{\Delta t\to 0}\frac{N_3(t+\Delta t) + N_2(t+\Delta t) - N_2(t) - N_1(t)}{\Delta t}$$

$$= \lim_{\Delta t\to 0}\left[\frac{N_2(t+\Delta t) + N_1(t+\Delta t) - N_2(t) - N_1(t)}{\Delta t} + \frac{N_3(t+\Delta t) - N_1(t+\Delta t)}{\Delta t}\right]$$

$$= \int_{cv}\frac{\partial}{\partial t}(\eta\rho)\mathrm{d}V + \lim_{\Delta t\to 0}\frac{1}{\Delta t}\left\{\int_{A_3}\eta\rho(\mathbf{u}_b\cdot\mathbf{n})\,\mathrm{d}A\Delta t - \int_{A_1}\eta\rho(-\mathbf{u}_b\cdot\mathbf{n})\mathrm{d}A\Delta t\right\}$$

$$= \int_{cv}\frac{\partial}{\partial t}(\eta\rho)\mathrm{d}V + \int_{cs}\eta\rho\,(\mathbf{u}_b\cdot\mathbf{n})\,\mathrm{d}A, \tag{10}$$

where $\mathbf{u}_b$ is the velocity of the control surface during the time from t to $t + \Delta t$ in Figure 3, and indicates the motion of control volume. For a non-deformable control volume, $\mathbf{u}_b$ is everywhere zero and the control volume is fixed in space.

Equation (9) above can be arranged by substituting equation (10) into

$$\frac{\mathrm{D}(N_{sys})}{\mathrm{D}t} = \int_{cv}\frac{\partial}{\partial t}(\eta\rho)\,\mathrm{d}V + \int_{cs}\eta\rho(\mathbf{u}_b\cdot\mathbf{n})\,\mathrm{d}A + \int_{cs}\eta\rho(\mathbf{u}_r\cdot\mathbf{n})\,\mathrm{d}A$$

$$= \int_{cv}\frac{\partial}{\partial t}(\eta\rho)\,\mathrm{d}V + \int_{cs}\eta\rho(\mathbf{u}\cdot\mathbf{n})\,\mathrm{d}A, \tag{11}$$

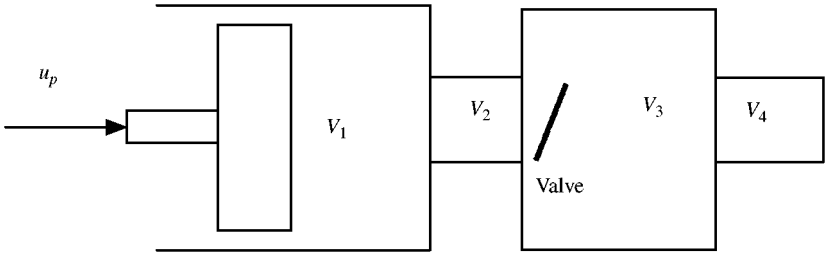

Figure 5. PC (piston–cylinder) model as a deformable control volume.

where $\mathbf{u}$ is the total velocity of the fluid with respect to the chosen reference frame in Figure 3, $\mathbf{u} = \mathbf{u}_r + \mathbf{u}_b$, during the time from the control volume at t to the system at $t + \Delta t$, and thus represents the boundary velocity of the system.

To get the motion equation, choose $\eta = \mathbf{u}$ as dividing a momentum with a mass, then equation (11) above is transformed as

$$\sum F = \int_{cv} \frac{\partial}{\partial t}(\rho \mathbf{u})\,\mathrm{d}V + \int_{cs} \rho \mathbf{u}(\mathbf{u}_b \cdot \mathbf{n})\,\mathrm{d}A + \int_{cs} \rho \mathbf{u}(\mathbf{u}_r \cdot \mathbf{n})\,\mathrm{d}A. \tag{12}$$

2.2. APPLICATION OF MOTION EQUATION ON COMPRESSOR MODEL

The equivalent model, piston–cylinder of compressor as a deformable control volume, is introduced in Figure 5. This PC model is illustrated in Figure 5 can be interpreted as consisting of two cavities, namely the cylinder V_1 and the muffler V_3, and of two necks, namely the clearance volume V_2 and the muffler discharge hole V_4. (A list of nomenclature is given in Appendix B.)

Subscripts denote the component position of cavities and necks. V means a cavity, u is velocity, ρ is density and A is an effective area. At this PC model, volume of cavity V_1 is not constant due to the movement of the rolling piston which has velocity u_p.

In this paper, in order to include the gas inertia due to decrease in the volume, the motion equation in the cavity V_1 has to be rearranged using equation (12). In the application of equation (12), it is necessary to define the boundary and relative velocity using the PC model in Figure 5.

$$\mathbf{u}_b = u_p, \qquad \mathbf{u}_r = u_2, \tag{13a, b}$$

where u_p is the velocity of a rolling piston in a rotary compressor, and is calculated by dividing the time derivative of a volume with a section area of the roller, $2R_R H_C$ as shown in Figure 2.

Our new proposed motion equation including the gas inertia term therefore can be obtained by substituting equations (13a, b) into equation (12). The revision of equation (12) gives

$$\frac{\partial}{\partial t}(\rho \mathbf{u})V + \rho \mathbf{u}(\mathbf{u}_b \cdot \mathbf{n})A + \rho \mathbf{u}(\mathbf{u}_r \cdot \mathbf{n})A = \sum F. \tag{14}$$

First and second terms in equation (14) are described using equation (13a, b) in the case of cavity V_1 of the PC model in Figure 5.

$$\frac{\partial}{\partial t}(\rho \mathbf{u})V = \frac{\partial}{\partial t}\left\{\rho_1 \frac{1}{2}|u_p + u_2|\right\} V_1, \tag{15a}$$

$$\rho \mathbf{u}(\mathbf{u}_b \cdot \mathbf{n}) A_1 = \rho_1 \left\{ \frac{1}{2} | u_p + u_2 | \right\} \dot{V}_1, \tag{15b}$$

where $A_1 = 2 R_R H_C$, $\mathbf{u}_b A_1 = \dot{V}_1$.

The third term in equation (14) can also be represented as below by the relations, $\mathbf{u}_b = 0$ and $\mathbf{u}_r = \mathbf{u}_2$, since this term indicates the exit of a cavity V_1 which does not have the moving velocity of control volume boundary.

$$\rho \mathbf{u}(\mathbf{u}_r \cdot \mathbf{n}) A_2 = \rho_2 u_2 | u_2 | A_2. \tag{16}$$

2.2.1. *The equation of motion in the neck V_1*

Therefore, equation (14) can be altered using equations (15) and (16), applying conservation of momentum to the first control volume V_1.

$$\frac{\mathrm{d}}{\mathrm{d}t} \left\{ \rho_1 V_1 \frac{1}{2} | u_p + u_2 | \right\} + \rho_2 u_2 | u_2 | A_2 = (P_1 - P_{r1}) A_2, \tag{17}$$

where P_{r1} is the entrance pressure of a neck V_2 in the PC model, and $P_1 - P_{r1}$ means therefore the pressure change across the exit of a control volume V_1.

However, the conventional NHR method describes the motion equation in the cavity V_1 as another different equation instead of equation (17), since conventional NHR method states that the effect of a gas inertia is negligible on the assumption that the volume of a cavity is larger than that of a neck.

$$\rho_2 u_2 | u_2 | A_2 = (P_1 - P_{r1}) A_2. \tag{18}$$

2.2.2. *The equation of motion in the neck V_2*

Since the gas in the neck is considered to be incompressible according to NHR assumption, it can be treated as a rigid body for a given time step, and Newton's second law of motion may be applied in th neck V_2.

$$\frac{\mathrm{d}}{\mathrm{d}t} (\rho_2 V_2 | u_2 |) = (P_{r1} - P_3) A_2. \tag{19}$$

This description of a neck is the same since the assumption of MNHR and NHR methods are coincident.

2.2.3. *The equation of motion on MNHR approach*

Our proposed MNHR approach gives the following equation by adding equation (17) in the cavity V_1 and equation (19) in the neck V_2.

$$\frac{\mathrm{d}}{\mathrm{d}t} \left\{ \rho_1 V_1 \frac{1}{2} | u_p + u_2 | \right\} + \rho_2 u_2 | u_2 | A_2 + \frac{\mathrm{d}}{\mathrm{d}t} (\rho_2 V_2 | u_2 |) = (P_1 - P_3) A_2. \tag{20}$$

From equation (20), the time derivative of fluid velocity $\dot{u}_2$ in the neck of V_2 gives

$$\begin{aligned} |\dot{u}_2| = & -\frac{1}{(\rho_2 V_2 + \frac{1}{2} \rho_1 V_1)} \left\{ \dot{\rho}_1 V_{1\frac{1}{2}} | u_p + u_2 | + \rho_1 \dot{V}_{1\frac{1}{2}} | u_p + u_2 | \right. \\ & \left. + \rho_1 V_{1\frac{1}{2}} | \dot{u}_p | + \dot{\rho}_2 V_2 | u_2 | + \rho_2 \dot{V}_2 | u_2 | + \rho_2 u_2 | u_2 | A_2 - (P_1 - P_3) A_2 \right\}. \end{aligned} \tag{21}$$

The sign of velocity u indicates a negative value in case of inflow, and a positive value in outflow.

A limiting condition is that u_2 has to be less than or equal to the speed of sound corresponding to the upstream temperature. When u_2 is equal to the speed of sound, ρ_1 of equation (25) described below applies alone until the density has dropped sufficiently to give subsonic speeds.

After subsonic speed is attained, both equations (21) and (25) apply.

2.2.4. *The equation of motion of NHR approach*

NHR describes the following motion equation by adding equation (18) and equation (19).

$$\frac{\mathrm{d}}{\mathrm{d}t}(\rho_2 V_2|u_2|) + \rho_2 u_2|u_2|A_2 = (P_1 - P_3)A_2. \tag{22}$$

Rearranging equation (22) also gives

$$|\dot{u}_2| = \frac{1}{\rho_2 V_2}\{ -\dot{\rho}_2 V_2|u_2| - \rho_2 \dot{V}_2|u_2| - \rho_2 u_2|u_2|A_2 + (P_1 - P_3)A_2\}. \tag{23}$$

The difference between our proposed MNHR and conventional NHR are explained by comparing equations (21) and (23): MNHR contains the density ρ_1, the volume V_1 and time derivative of volume $\dot{V}_1$ in a compressor cylinder. And the velocity u_p and acceleration $\dot{u}_p$ of a rolling piston is also included. However conventional NHR ignored these parameters. These differences between them are compared and analyzed next using numerical and experimental results.

2.2.5. *The continuity equation of the cavity* V_1

Applying the conservation of mass for the cavity V_1 in Figure 5, gives

$$\frac{\mathrm{d}}{\mathrm{d}t}(\rho_1 V_1) + \rho_2 u_2 A_2 = 0, \tag{24}$$

where $\rho_1 V_1$ is the mass in volume V_1, ρ_2 and u_2 is the mass density and the gas velocity of the neck V_2 respectively. Contraction and velocity profile effects are assumed to be included in the effective flow area A.

Rearranging equation (24) yields the time derivative of a density $\dot{\rho}_1$ of the cavity V_1,

$$\dot{\rho}_1 = -\frac{1}{V_1}(\rho_1 \dot{V}_1 + \rho_2 u_2 A_2). \tag{25}$$

2.2.6. *The continuity equation of the cavity* V_3

In a similar manner as before, the conventional NHR used for the control volume V_1 and V_2 is applied to the control volume V_3 and V_4, since a volume of the cavity V_3 does not change unlike V_1.

The continuity equation of V_3 takes the inflow and outflow velocities as follows:

$$\frac{\mathrm{d}}{\mathrm{d}t}(\rho_3 V_3) - \rho_2 u_2 A_2 + \rho_4 u_4 A_4 = 0. \tag{26}$$

The time derivative of density $\dot{\rho}_3$ is also given as

$$\dot{\rho}_3 = \frac{1}{V_3}\,(-\rho_3\dot{V}_3 + \rho_2 u_2 A_2 - \rho_4 u_4 A_4). \tag{27}$$

2.2.7. *The equation of motion in the neck* V_4

If the same process is applied to the neck V_4, by adding the momentum equation of the cavity V_3 to that of the neck V_4, and by assuming negligible compressible effect of gas, a motion equation is obtained as follows:

$$\frac{\mathrm{d}}{\mathrm{d}t}(\rho_4 V_4 |u_4|) + \rho_4 u_4 |u_4| A_4 = (P_3 - P_5)A_4, \tag{28}$$

where P_5 indicates the ambient or the final pressure of a terminal point in the last control volume of PC model.

Rearranging the equation (28) above gives

$$|\dot{u}_4| = -\frac{1}{\rho_4 V_4}\,\{\dot{\rho}_4 V_4 |u_4| + \rho_4 \dot{V}_4 |u_4| + \rho_4 u_4 |u_4| A_4 - (P_3 - P_5)A_4\}. \tag{29}$$

2.2.8. *The density of necks* V_2 and V_4

Conventional CHR implies that the density of the assumed incompressible plug of gas is equal to the mean flow density. All densities are therefore replaced by a constant value since CHR assumes that amplitude of pressure and velocity is small.

However, NHR states that the density of the neck is equal to an average of the densities in the two adjoining cavities in PC model.

$$\rho_2 = \frac{(\rho_1 + \rho_3)}{2}, \qquad \rho_4 = \frac{(\rho_3 + \rho_5)}{2}. \tag{30a, b}$$

2.2.9. *The pressure of cavities* V_1 *and* V_3

To relate pressure to mass changes and heat transfer, the first law of thermodynamics could be used. However, compressor designers have traditionally used the polytropic process, since the two descriptions are equivalent if one assumes that the heat transfer plus convected energy is proportional to external work [7]. Using a polytropic process description, one obtains

$$P_1 = P_{10}\left(\frac{\rho_1}{\rho_{10}}\right)^n, \qquad P_3 = P_{30}\left(\frac{\rho_3}{\rho_{30}}\right)^n, \tag{31a, b}$$

where superscript n means polytropic index, the subscript 0 denotes initial values.

2.3. ROLE AND EXISTENCE OF A COMPRESSOR VALVE

To describe the fluid flow during operation in an actual compressor, a valve motion must be taken into account, because a gas pulsation or unsteady flow has a relation with the periodical valve motion.

A valve in a compressor controls the flow of refrigerant gas: when the pressure of compressed gas is higher than that of discharged gas, it opens and discharges a gas; and it

TABLE 1

Modelling of valve existence of PC model

	$P_1 \leqslant P_3$	$P_1 > P_3$
Quasi-steady (QS) $\dot{m}_2$	0	Table A1
New Helmholtz (NHR) $\dot{u}_2$	0	Equation (23)
Modified New Helmholtz (MNHR) $\dot{u}_2$	0	Equation (21)

TABLE 2

Geometrical data of PC model for numerical analysis

Volume/effective area/ effective length	Spec
V_1 (cm^3)	17·075
A_2 (cm^2)	0·567
L_2 (cm)	0·37
V_3 (cm^3)	21
A_4 (cm^2)	0·331
L_4 (cm)	0·15

closes in the opposite case. A valve protects the incoming back-flow of a discharged gas stayed at the muffler during the compression stage. In an actual valve motion, there is a time delay due to the interaction between the valve motion and the fluid flow around the valve. A lot of papers describing the valve motion under the influence of fluid flow were presented, with special attention to the stopper or the retainer [8, 9].

The main object of this paper is to propose a new calculation method by considering a gas inertia effect due to decreasing volume of a cavity, which happens at a compressor cylinder in an actual operation of compressor. The effect of valve motion affecting fluid flow is therefore ignored, only to compare the pressure calculation method mentioned above. We assume that fluid flow is generated only from pressure difference between the upstream and the downstream sides, and not affected by an interference due to valve motion. Time delay in fluid motion due to a valve displacement is thus not included in this calculation process.

For the modelling of an ideal valve existence of PC model in Figure 5, an assumption of Table 1 is adopted. A role of an ideal valve can be defined with a comparison of pressures between a cavity V_1 and V_3. If P_1, pressure of a cavity V_1, is less than or equal to P_3, pressure of a cavity V_3, then fluid does not flow. On the contrary, if P_1 is greater than P_3, then fluid flows and this case indicates the valve open state.

2.3.1. *Geometrical data of PC model*

For the numerical analysis, geometrical data of PC model in Table 2 is used. These values are obtained from a real compressor under production. Cavities of V_1 and V_3 are the cylinder and the muffler respectively. Necks of V_2 and V_4 represent the clearance volume and the muffler discharge hole, and they have an effective area and an effective length.

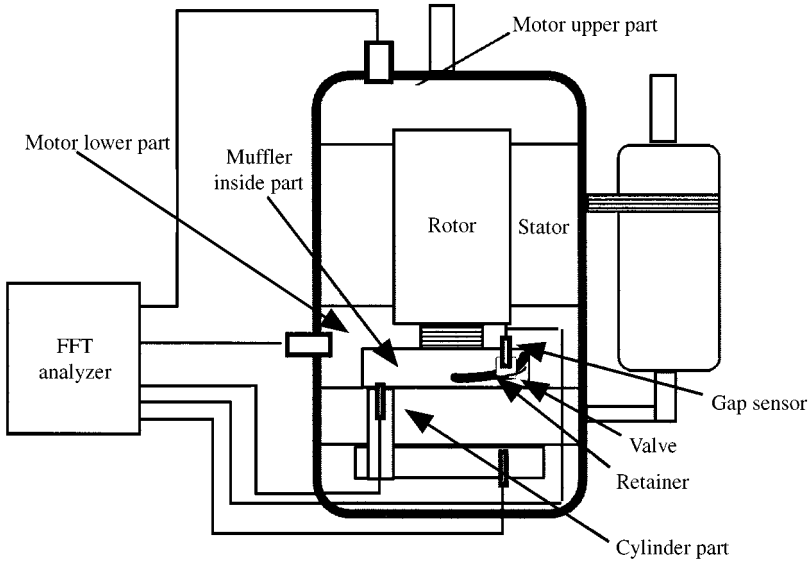

Figure 6. Schematic diagram of the modified compressor for measuring of pressure pulsation and valve lift.

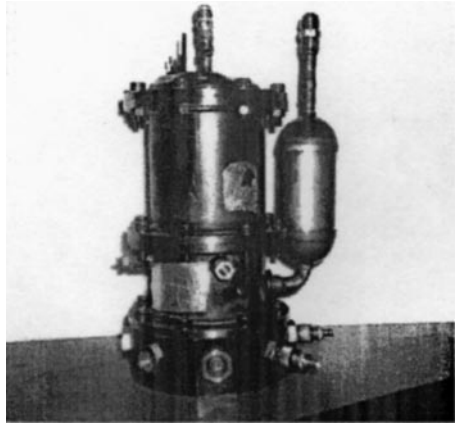

Photo 1. Test jig of modified compressor.

3. EXPERIMENT

A pressure pulsation under an actual compressor operating condition is measured, to compare our proposed MNHR with other conventional methods: QS and NHR. A test jig of a modified compressor in Figure 6 which has pressure transducers inside a compressor shell was fabricated, and the main key point of this apparatus is to overcome the technical difficulty of sensor attachment to the inside of the compressor shell.

Since the real compressor product is a shell made by heat press fit, it is not easy to disassemble the compressor shell for sensor installation at each part: upper and lower motor part, muffler inside and cylinder inside part, which are shown in Figure 6. Photo 1 shows the external view of this test jig of the modified compressor.

TABLE 3

Technical data of pressure transducer

	Charge relative
Manufacture	Kistler
Type	6051
Range	0–200 bar
Sensitivity	− 1·9 pC/bar
Natural frequency	200 kHz
Linearity	± 1% FSO
Temperature range	− 196–350°C
Amplifier	Charge amp.
Type	5011

Photo 2. Calorimeter for measuring compressor performance.

We choose the cylinder inside part as the measuring point of pressure, since this part experiences the abrupt pressure change from low to high state and this position thus is adequate to express our new proposed assumption appropriately. A sensor attachment position is near the discharging port as indicated in Figure 2. A specification of pressure transducer used for measuring pressure at this cylinder part is summarized in Table 3.

To measure the practical value of pressure under actual operating compressor with a refrigerant gas as a working fluid, a facility named a calorimeter was utilized, which measures compressor performance and has a secondary refrigerant system as an auxiliary cycle. Photos 2 and 3 display this calorimeter and test jig of modified compressor set-up in a calorimeter respectively.

Initial and boundary conditions follow the American Society of Heating, Refrigeration and Air-conditioning Engineers (ASHRAE) compressor test condition in the case of R22 freon gas, described in Table 4. For the numerical comparison, a cylinder V_1 has initial

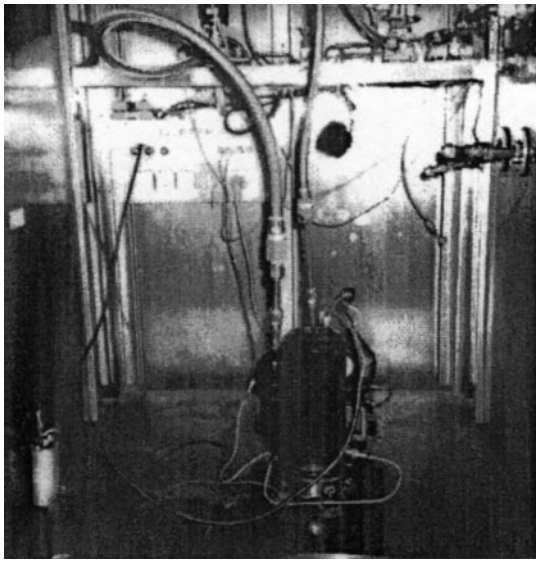

Photo 3. Test jig of modified compressor in a calorimeter.

TABLE 4

Compressor test condition

Pressure at suction	(kg/cm^2 A)	6·37
Pressure at discharge	(kg/cm^2 G)	20·86
Temperature at expansion valve	(°C)	46·1
Temperature at calorimeter outlet	(°C)	35·0
Temperature at calorimeter room	(°C)	35·0
Temperature at compressor room	(°C)	35·0
Temperature at suction	(°C)	35·0
Voltage	(V)	220
Frequency	(Hz)	60

values of the pressure P_1 and density ρ_1 at suction side, ambient boundary values of discharge side also has P_5 and ρ_5 is indicated in PC model in Figure 5.

4. RESULTS AND DISCUSSIONS

Experimental and numerical results are obtained for comparison of pressure calculation methods between the MNHR and conventional methods: QS and NHR.

Density oscillation of cavities 1 and 3, that is, a compressor cylinder and a muffler, are shown in Figures 7 and 8 respectively. Their pressure oscillations are also presented in Figures 9 and 10.

The present method describes the over-compression phenomena, at the instant of valve opening, of cavity 1 in Figures 7 and 9, which is not obtained by other conventional

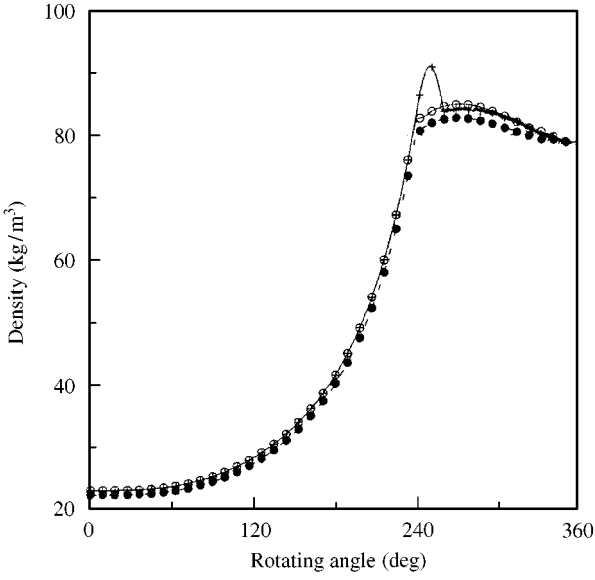

Figure 7. Density oscillation in volume 1 (compressor cylinder) of PC model; —○—, new Helmholtz; (—●—), quasi-steady; (—┼—), present.

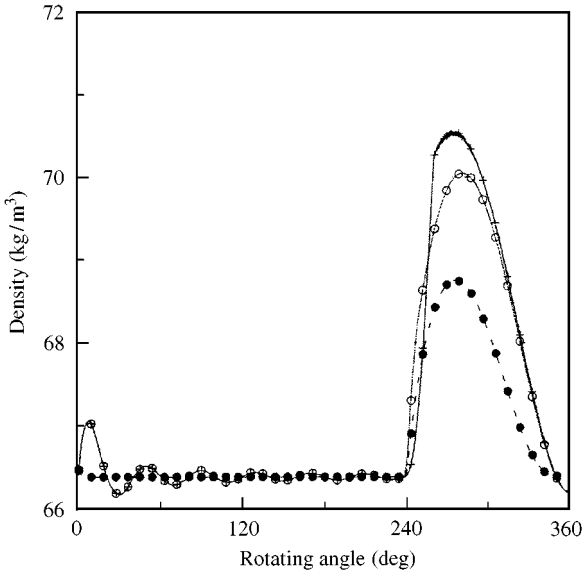

Figure 8. Density oscillation in volume 3 (muffler) of PC model: —○—, new Helmholtz; (—●—), quasi-steady; (—┼—), present.

methods: QS and NHR. This means that our proposed present method has a unique characteristic in predicting pressure variation in cavity 1 due to volume decrease according to piston movement of PC model in Figure 5.

This difference between MNHR and conventional methods (QS and NHR) are due to our new assumption that the gas inertia has to be included in cavities of classical Helmholtz

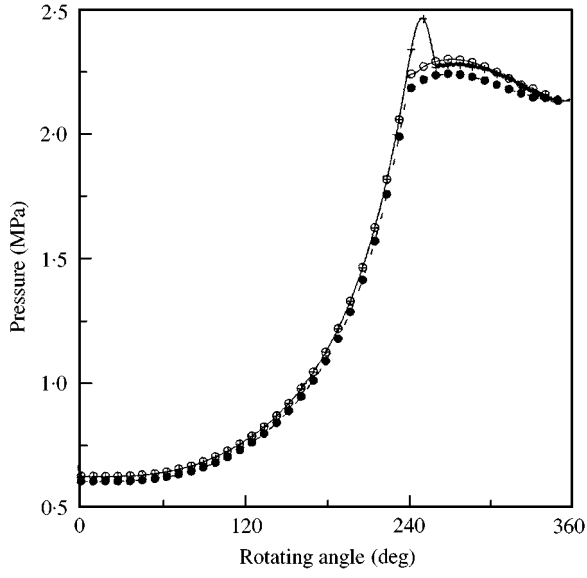

Figure 9. Pressure oscillation in volume 1 of PC model: —○—, new Helmholtz; (—●—), quasi-steady; (—┼—), present.

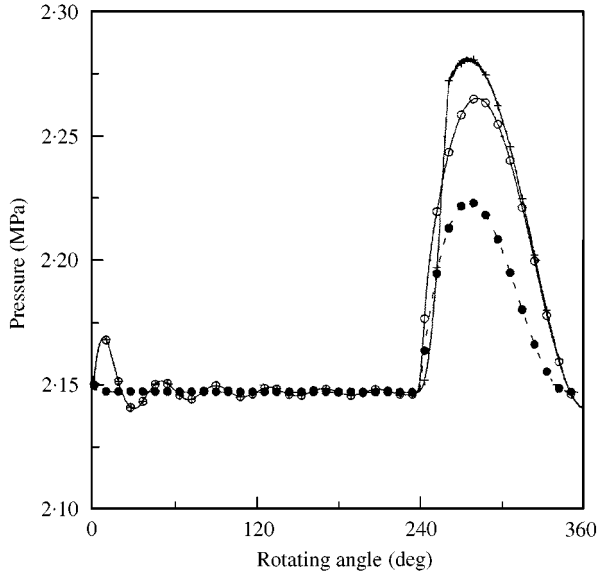

Figure 10. Pressure oscillation of volume 3 of PC model: —○—, new Helmholtz; (—●—), quasi-steady; (—┼—), present.

resonator model when the volume of cavities such as compressor cylinder decreases due to a rolling-piston movement.

Density and pressure oscillations in cavity 3 show no significant difference between our new MNHR and conventional NHR. This implies that these methods are based on the same assumption that the gas inertia is negligible when the volume of cavity does not change.

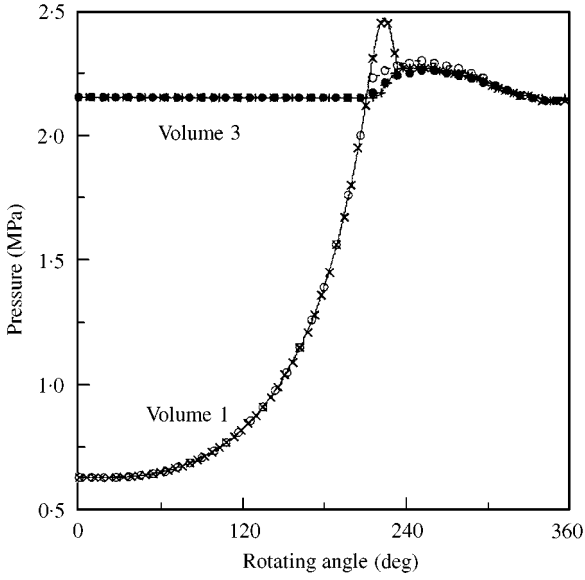

Figure 11. Pressure oscillation in volume 1 and 3 of PC model: —○—, new Helmholtz (P1); (—×—), present (P1); (—●—), new Helmholtz (P3); (—+—), present (P3).

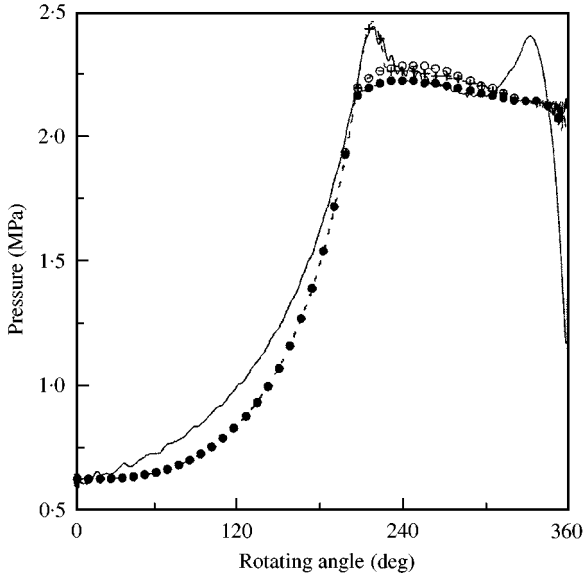

Figure 12. Pressure in cylinder by various numerical models and experimentation: —○—, new Helmholtz; (—●—), quasi-steady; (—+—), present; (——), experiment.

Comparison of P_1 and P_3 in Figure 11 shows that the pressure results of all approaches are the same before the discharge valve opens at about 210° of rotating angle. The pressures of the valve opening by all approaches shown similar results.

Validity of the newly proposed MNHR method is assured by comparing the calculation results to the experimental results as presented in Figure 12 and in detailed scale in Figure 13.

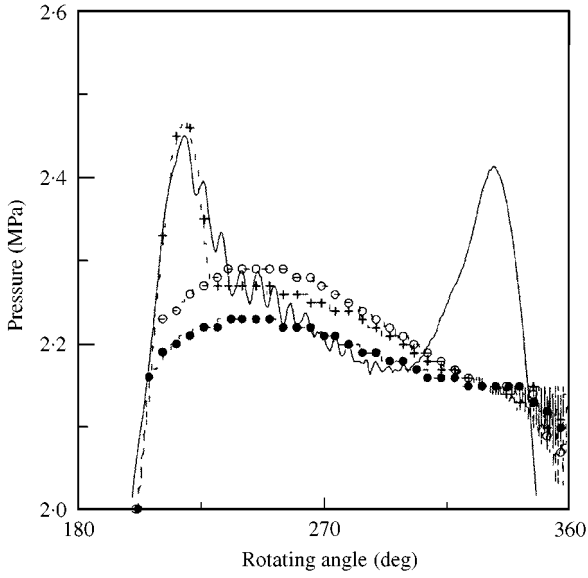

Figure 13. Pressure at detailed scale in cylinder right after the valve opening by numerical models experimentation: —○—, new Helmholtz; (—●—), quasi-steady; (+), present; (—+—), experiment.

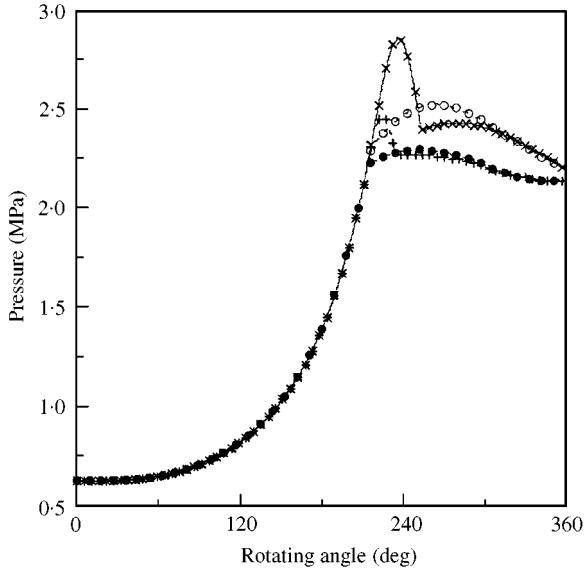

Figure 14. Comparison of pressure in volume 1 of PC model due to operating velocities: —○—, new Helmholtz (120 Hz); (—×—), present (120 Hz); (—●—), new Helmholtz (60 Hz); (—+—), present (60 Hz).

Only our MNHR method follows the over-shooting phenomena at an instant of valve opening depicted by the experimental results. The difference between the experimental result and numerical ones before the valve opening shown in Figure 12 can be explained by the fact that the gradient of pressure increase depends on the polytropic index n, which ignores the heat transfer at compressor cylinder structure.

Another difference between the numerical and experimental result at the end of one cycle means that this is developed from the simplification of a real complicated flow mainfold, and from the error inevitable in a pressure transducer installation. Other reasons can be found in ignoring the leakage consideration in the simplified PC model. All calculation methods including our MNHR, conventional QS and NHR have a restriction in describing the pressure surging at the end of one cycle.

When the compressor operation speed is increased, for example, in an inverter drive air-conditioner, the gas inertia effects have to be included. The profile of Figure 14 shows that the difference between our MNHR and convention NHR becomes larger as the operation speed is doubled.

5. CONCLUSIONS

The pressure pulsation in refrigerant compressor has been studied by various methods. A new pressure calculation method is proposed to include the gas inertia due to a decrease in the volume of cavity in the conventional Helmholtz resonator model by a rolling piston movement. The comparisons with an experimental result show that the proposed MNHR is better than other conventional QS or NHR in predicting pressure over-shooting phenomena at an instant of valve opening state.

ACKNOWLEDGMENT

This work was supported by the Korea Research Foundation Grant.

REFERENCES

1. T. YANAGISAWA and T. SHIMIZU 1982 *Proceedings of Purdue Compressor Technology Conference*, 185–192. Motion analysis of rolling piston in rotary compressor.
2. W. SOEDEL 1972 *Purdue University Short Course Text*. Introduction to Computer Simulation of Positive Displacement Compressor.
3. W. SOEDEL and E. P. NAVAS 1973 *Journal of Sound and Vibration* **30**, 263–277. On Helmholtz resonator effects in the discharge system of a two-cylinder compressor.
4. V. YEE 1982 *Ph.D. Thesis, Purdue University*. Analytical and experimental study of high speed rotary vane sliding vane compressor dynamics with application to transfer slot design.
5. V. YEE and W. SOEDE 1983 *Journal of Sound and Vibration* **91**, 27–36. Pressure oscillations during re-expansion of gases in rotary vane compressors by a modified Helmholtz resonator approach.
6. M. C. POTTER and J. F. FOSS 1975 *Fluid Mechanics*. New York: Ronald.
7. J. F. HAMILTON 1974 *Purdue University Short Course Text*. Extension of mathematical modelling of positive displacement type compressors.
8. K. H. REDDY 1974 *Ph.D. Thesis, Purdue University*. Computer simulation of a reciprocating compressor with special emphasis on the prediction of dynamic strains in ring type valves.
9. Y. C. MA and J. Y. BAE 1996 *Proceedings of Purdue Compressor Technology Conference*, 371–376. Determination of effective force area and valve behaviour on the rolling piston type compressor.

APPENDIX A

The general calculation method of the pressure of a cylinder is a quasi-steady flow equation. The relations are shown in Table A1.

TABLE A1

Mass flow rate using quasi-steady flow equation[†]

	$P_u > P_d$	$P_u < P_d$
Mass flow rate, $\dot{m}$	$\dot{m} = P_u A \sqrt{\frac{2k}{(k-1)RT_u}(S^{2/k} - S^{k+1/k})}$	$\dot{m} = -P_d A \sqrt{\frac{2k}{(k-1)RT_d}(S^{2/k} - S^{k+1/k})}$
Pressure ratio, S	$S = R_i$ if $R_i > r_c$ $S = r_c$ if $R_i \leqslant r_c$ $r_c = \left(\frac{2}{k+1}\right)^{k/k-1}$: critical pressure ratio k: specific heat ratio	
R_i	$R_i = \frac{P_d}{P_u}$	$R_i = \frac{P_u}{P_d}$

[†] Subscript denotes (u) upstream, (d) downstream.

APPENDIX B: NOMENCLATURE

Alphabetic symbols

A	area of neck
b	vane thickness
c	sound speed of refrigerant gas
D	diameter of discharge port
e	relative eccentricity, $R_C - R_R$
H_c	cylinder height
L	effective length of neck
m	mass of fluid
N	extensive property
P	pressure
P_{r1}	inlet pressure of neck 2
$\Delta P(t)$	pressure difference around valve system
R_V	vane tip radius
R_R	roller radius
R_C	cylinder radius
R	gas constant
t	time
$\mathbf{u}$	velocity of fluid element
$\mathbf{u}_b$	velocity of control volume boundary (control surface)
$\mathbf{u}_r$	relative velocity with respect to control volume boundary element
V	volume of capacity
V_T	total volume of cylinder
$\mathbf{w}$	velocity of fluid

Greek symbols

η	intensive property
χ	vane extension
k	specific heat ratio of refrigerant gas
ρ	density of fluid
θ	rotation angle of crank-shaft

ω	rotating velocity of crank-shaft
δ	difference between valve lift and retainer height, $y(x) - R(x)$

superscript

n	polytropic index

subscript

c.v.	control volume
c.s.	control surface
d	downstream
sys	system
u	upstream
0	initial condition